Journal of Hydrology: Regional Studies 50 (2023) 101541

Contents lists available at ScienceDirect

Journal of Hydrology: Regional Studies

journal homepage: www.elsevier.com/locate/ejrh

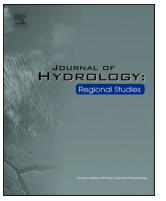

Multi-source remote sensing data and image fusion technology reveal significant spatiotemporal heterogeneity of inundation dynamics in a typical large floodplain lake system

Xuchun Ye [a,b], Juan Wu [a], Xianghu Li [c,1,*], Yunliang Li [c], Qi Zhang [d], Chong-Yu Xu [e]

[a] Chongqing Key Laboratory of Karst Environment & School of Geographical Sciences, Southwest University, Chongqing 400715, China
[b] Chongqing Jinfo Mountain Karst Ecosystem National Observation and Research Station, Chongqing 400715, China
[c] Nanjing Institute of Geography and Limnology, Chinese Academy of Sciences, Nanjing 210008, China
[d] Yangtze Institute for Conservation and Development, Hohai University, Nanjing 210024, China
[e] Department of Geosciences, University of Oslo, N-0316 Oslo, Norway

ARTICLE INFO

Keywords:
Floodplain lake
Remote sensing
Image fusion model
Dish-shaped lake
Stage-area relationship

ABSTRACT

Study region: The Poyang Lake, which is located on the south bank of the middle-lower Yangtze River basin. The lake is the largest freshwater lake in China, and also a typical floodplain lake in the world.
Study focus: The spatiotemporal heterogeneity of inundation dynamics of large floodplain lake system has not been paid enough attention. Based on the reconstructed high spatial and temporal resolution inundation dataset using the image fusion model and multi-source remote sensing data, this study systematically analyzed the spatiotemporal heterogeneity of inundation dynamics in the Poyang Lake- floodplain system.
New hydrological insights for the region: It is found that within the same floodplain lake, the inundated area and inundation frequency in different regions of the lake (the main lake region and the adjacent floodplain region) can have asynchronous intra-annual fluctuation and opposite inter-annual change trend. This is highly related to the hydrological complexity of the lake: the relative impacts of catchment inflow and the Yangtze River varies in different regions across the lake. The stage-area relationship at the central station along the flow direction of the lake has the highest linear correlation, which might provide more accurate estimates of lake surface/volume. In addition, this study highlights the importance of reconstructed high spatial-temporal resolution of remote sensing data for the accurate assessment of inundation dynamics in floodplain lakes. All the results enrich the understanding of complex hydrological regime of large floodplain lakes and are valuable for the practice of water resources management and ecological conservation in such lakes.

1. Introduction

Lakes and other periodically inundated floodplains constitute the most diverse ecosystems on the Earth, which play an

* Correspondence to: Nanjing Institute of Geography and Limnology, Chinese Academy of Sciences, 73 East Beijing Road, Nanjing 210008, China.
E-mail address: xhli@niglas.ac.cn (X. Li).
[1] ORCID: 0000-0001-9934-1822

https://doi.org/10.1016/j.ejrh.2023.101541
Received 6 April 2023; Received in revised form 27 September 2023; Accepted 1 October 2023
Available online 5 October 2023

irreplaceable role in regulating river runoff, reducing drought and flood disasters and providing water resources and biological habitat (Heimhube et al., 2017; Li et al., 2019b; Zhang et al., 2023). For the lake ecosystem, changes in lake inundation conditions play an important role in the formation and evolution of wetland vegetation, and affect the quality of fish and wildlife habitats (Zedler and Kercher, 2005; Allen, 2016; Tan et al., 2016; Li et al., 2021). Among many variables, the lake area is one of the basic parameters for the understanding of lake hydrology and morphology. Variation of lake surface responses to catchment water balance which in turn is controlled by climate and environmental change (Gronewold et al., 2016; Frappart et al., 2018; Ye et al., 2020). The inundation frequency reflects the duration and extent a lake is inundated/exposed during a specific time period, and is considered to be the most essential hydrological factor affecting the structure and function of the lake ecosystem (Casanova and Brock, 2000). Investigation of spatiotemporal variations of inundation dynamics is of great significance for maintaining water quantity, ecological integrity and promoting management practices of the lake ecosystem.

Floodplain lakes are widely distributed in floodplain areas in the middle-lower reaches of large rivers, having outstanding significance to the water supply and eco-environmental maintenance (Yang et al., 2010). These lakes usually exhibit considerable seasonal water level fluctuations and time-varying boundaries, and are strongly affected by the effects of regional climate change and human disturbance (Coops and Hosper, 2002; Ye et al., 2020). Meanwhile, significant seasonal fluctuations of lake water levels and associated water surface lead to the formation of extensive floodplain wetlands in the transition zone formed by the expansion and contraction of the lake in flood season and dry season, respectively (Coops et al., 2003). With these unique features, floodplain lakes are normally characterized as a geographical unit of structural integrity, spatial heterogeneity, system openness, process complexity and ecological vulnerability (Hudon et al., 2006; Li et al., 2019a; b; Zhang and Werner, 2015).

Exploring inundation dynamics and water volume change of lakes has always been the concern of hydrologists all over the world. However, most of the previous studies mainly reported the long-term change trend of inundation dynamics (such as water level, water

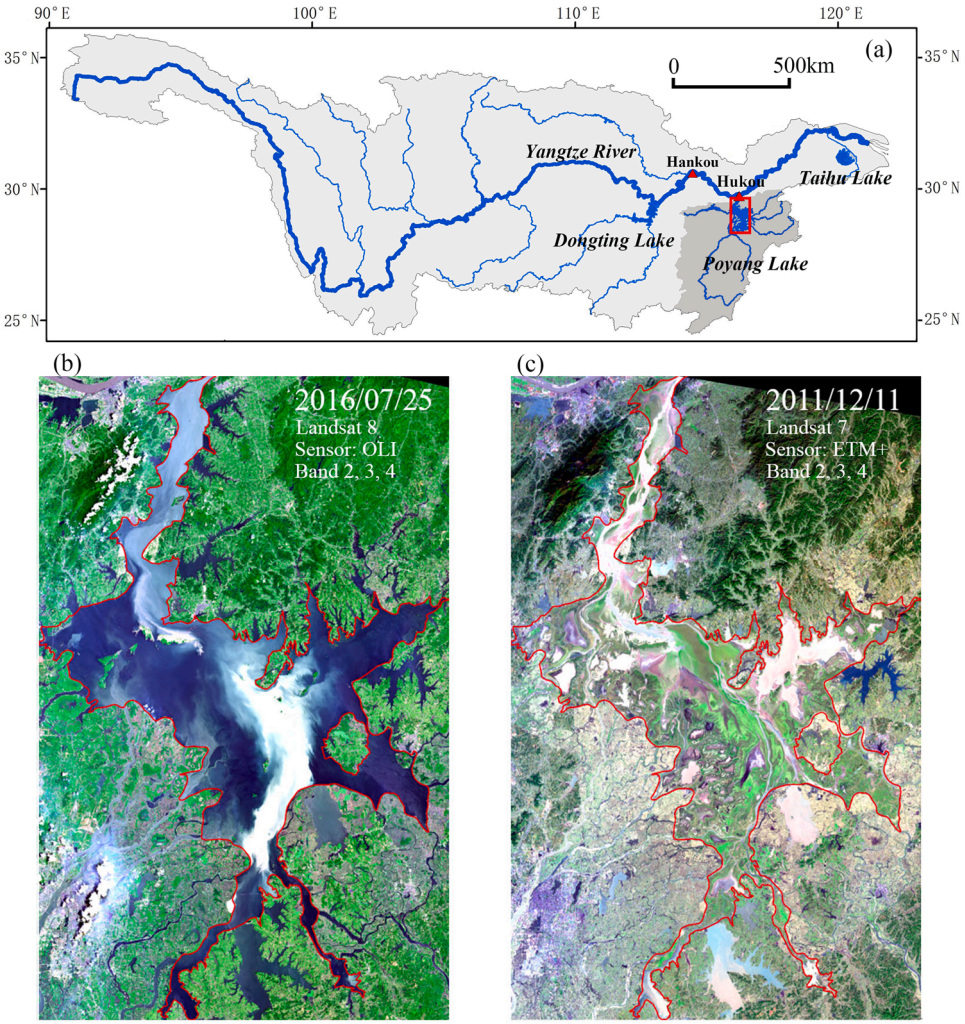

Fig. 1. (a) location of the Poyang Lake and its catchment in the Yangtze River basin, (b) and (c) show the typical scenes of lake inundation during flood and dry periods.

surface and volume) from the perspective of the whole lake. For example, studies have shown that Victoria Lake in Africa (Sichangi and Makokha, 2017) and the Poyang Lake in China (Liu et al., 2013) are shrinking, while lakes on the Qinghai Tibet Plateau (Liu et al., 2021) and Great Lakes in North American (Gronewold and Rood, 2019) are expanding in recent years. Some studies have focused on the spatial-temporal change of inundation in floodplain lakes, but few have realized that there may be a simultaneous increase and decrease in the inundation area of different regions within the same lake (e.g. Hui et al., 2008; Wu and Liu, 2015). Due to highly spatial heterogeneous of morphology, bathymetric features and hydrodynamic conditions (Li et al., 2019b; Zhang et al., 2014), this spatial difference in inundation dynamics may be more pronounced between the main lake and adjacent floodplains in those floodplain lakes.

It is of interest to scientifically understand the spatiotemporal heterogeneity of inundation dynamics in floodplain lakes and the driving mechanisms behind them. However, there is still a lack of in-depth researches and clear conclusions on whether there exist asynchronous seasonal fluctuations and opposite change trends in inundation area of different regions within the same floodplain lake. The reasons for this knowledge gap are, on the one hand, a lack of understanding of the hydrological complexity of shallow floodplain lakes (Li et al., 2019b), and on the other hand, the methodological challenge of quantitative research (Wu and Liu, 2015). Because of the wide range of floodplain wetlands, traditional in situ investigation and gauge measurements are difficult to provide an overall pattern of lake inundation conditions on a regional scale due to low efficiency or sometimes inaccessible in some areas (Alsdorf et al., 2007). Numerical simulation has great advantages in meeting the research needs of hydrological and hydrodynamic processes at various time and spatial scales and future change prediction (Koponen et al., 2005; Rudorff et al., 2014; Li et al., 2014; Tan et al., 2022). Whereas, due to the limitation of designed lake boundary, the accuracy of varied lake bathymetry, and simplified model structure, uncertainties may widely exist in the numerical simulation of floodplain lakes (Li et al., 2014; Tan et al., 2019). Compared to traditional methods, remotely sensed observations offer a unique opportunity to detect inundation dynamics of large-scale water surface with high accuracy (Cazenave et al., 2004; Tan et al., 2020; Wu and Liu, 2015). However, the remote sensing products from the same satellite sensor are difficult to be reconciled in terms of high spatial resolution and high revisit frequency (Price, 1994). As a result, for those floodplain lakes that suffering rapid and significant short-term lake water level fluctuation, the biggest disadvantage of using remote sensing approach in monitoring the inundation dynamics lies in the acquisition of continuous images with both high spatial resolution and frequent coverage (Ye at al, 2019; Tan et al., 2020).

The Poyang Lake, located in the middle and lower reaches of the Yangtze River, is the largest freshwater lake in China (Fig. 1a). The lake receives water from its catchment in the south and flows into the Yangtze River in the north, forming a complete catchment-lake-river water system. It is a typical large shallow lake ecosystem in subtropical monsoon climate zone and an internationally representative floodplain wetland (Yao et al., 2016; Ye et al., 2019). The combined effect of catchment inflows and the interaction with the

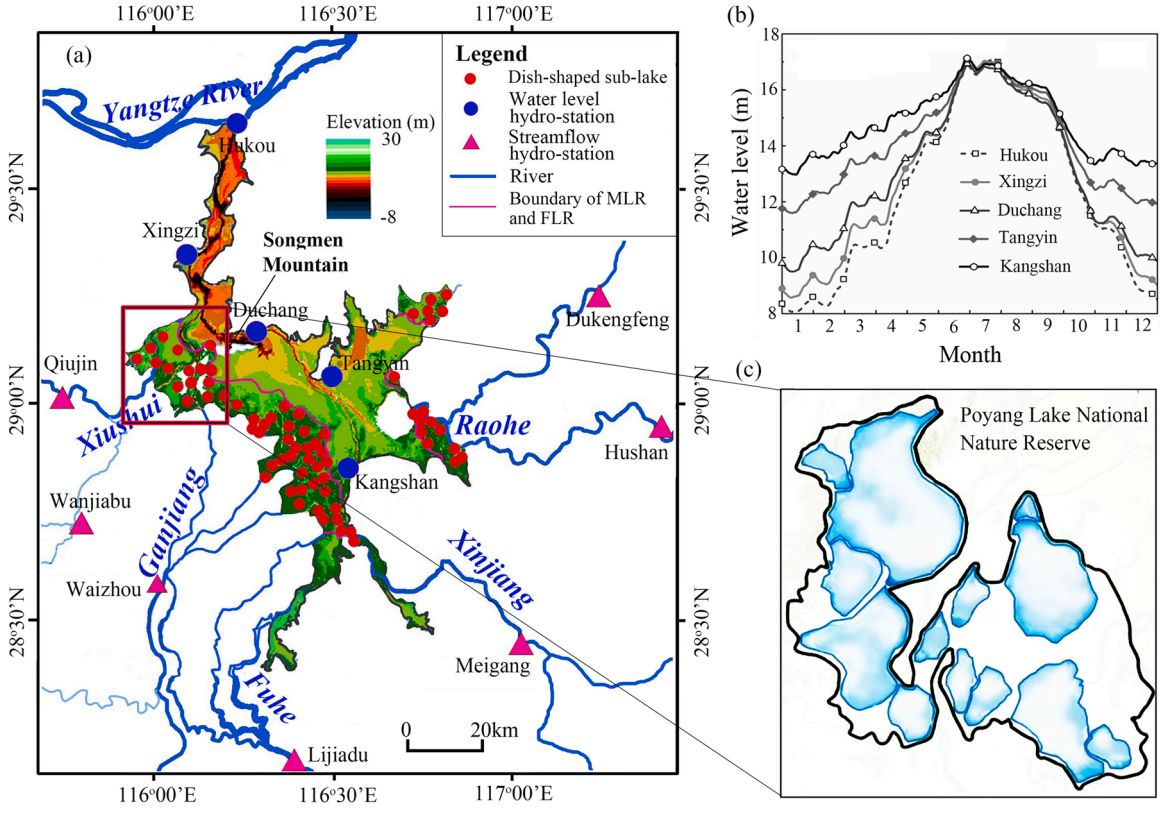

Fig. 2. Physical geographical features of the Poyang Lake: (a) composition of Poyang Lake water system; (b) intra-annual variation of water level of the main hydro-stations in the lake; (c) distribution of dish-shaped temporary lakes in the Poyang Lake National Nature Reserve.

Yangtze River results in a considerable seasonal variation of 10 m in the lake water levels (Zhang and Werner, 2015). This remarkable fluctuation of water level forms the extremely rare scene of wetland landscape in global freshwater lakes: a boundless ocean in flood season while a narrow meander in dry season (Figs. 1b, 1c). The lake ecosystem provides vital natural habitats for the largest concentrations of fish stocks and migratory birds in East Asia (Finlayson et al., 2010). In recent years, the extreme change of the hydrological regime of the Poyang Lake is obvious, which has inevitably caused threat and damage to the wetland ecosystem, causing profound impacts on the water resources security and ecological protection in the middle and lower reaches of the Yangtze River (Li et al., 2019a; Tan et al., 2016; Ye et al., 2020).

The aim of this work is to investigate the spatiotemporal heterogeneity of inundation dynamics in a typical large floodplain lake system – the Poyang Lake in the Yangtze River basin. This was achieved by utilizing multi-source remote sensing data and image fusion technology to reconstruct a high spatiotemporal resolution inundation dataset. Spatiotemporal difference of the relationship between inundation dynamics and lake water level was further examined, and the driving mechanisms and significance behind the spatiotemporal heterogeneity of inundation dynamics in the floodplain lake system were also explored. Outcomes of this study will enrich the understanding of complex hydrological regime of large floodplain lakes and promote the management practice of lake ecosystem.

2. Materials and Methods

2.1. Overview of the study area

Poyang Lake is located on the south bank of the middle-lower Yangtze River. It is one of the few large lakes that remains naturally connected to Yangtze River. The lake has a gourd shaped outline with irregular shoreline. The lake terrain topography varies from 30 m in the floodplain regions to − 8 m in the flow channels (Fig. 2a). The lake is a typical shallow lake with 85% of the water depth < 6 m during flood seasons, while the maximum depth can reach 30 m downstream of the lake's outflow channels (Li et al., 2017).

The whole drainage basin of the lake is about 162, 225 km^2 and average annual streamflow is about 1450×10^8 m^3, which account for 9% and 15% of the area and water volume of the Yangtze River basin, respectively (Ye et al., 2012). Both the catchment inflow rivers and the Yangtze River play a combined effect on the lake water-level fluctuations between 8 and 22 m in a year (Li et al., 2017) (Fig. 2b). In the rainy season, the water level of the lake rises and lake water surface can expand to nearly 4000 km^2, while in the dry season, lake water level drops and water surface shrinks to less than 500 km^2 (Wu et al., 2017). This process creates an extensive floodplain areas of 3000 km^2 adjacent to main lake. In the lake floodplain regions, numerous interconnected dish-shaped temporary lakes are widely distributed with sizes ranging from 1 km^2 to 71 km^2 (Fig. 2a). Total water surface of these dish-shaped temporary lakes is about 767 km^2 (Tan et al., 2020). The shallow floodplains and dish-shaped temporary lakes play an important role in flood regulation and biodiversity conservation (Fig. 2c) (Liu et al., 2023). Based on the periphery distribution of dish-shaped temporary lakes, the whole lake was roughly divided into two parts in this study: the main lake region (MLR) and the floodplain temporary lakes region (FLR) (Fig. 2a).

2.2. Data acquisition

A total of 299 cloud-free Landsat images (including TM, ETM +, OLI) (downloaded from http://glovis.usgs.gov) and 847 MODIS surface reflectance products from NASA Terra platform (MOD09A1) (http://reverb.echo.nasa.gov) covering the study area during the period 2000–2020 were collected. Table 1 shows detailed information of multi-source remote sensing data in this study. The Landsat data have a spatial resolution of 30 m and temporal resolution of 16 d. The MOD09A1 data set is a composited product of 500 m surface reflectance of MODIS data every 8 days. Before application, all image data were subjected to standardized preprocessing on ENVI platform, including projection transformation, radiometric calibration and atmospheric correction.

Daily water levels from five hydro-stations (Hukou, Xingzi, Duchang, Tangyin and Kangshan) across the Poyang Lake and daily streamflow from seven hydro-stations (Qiujin, Wanjiabu, Waizhou, Lijiadu, Meigang, Hushan and Dufengkeng) of the five major inflow rivers were collected during the period 2000–2020. These data were used to measure spatial difference of lake water level and the inflow discharge from the lake catchment. Likewise, daily discharges from Hankou hydro-station during the period 2000–2018 were also collected to represent water flux from the upper-middle Yangtze River. All these hydrological data will help in understanding the background formation mechanism of the lake inundation processes.

2.3. Water surface extraction and inundation frequency calculation

The normalized difference water index (NDWI) (McFeeters, 1996) method was applied to extract inundated area (IA) of the Poyang

Table 1
Remote sensing images used in this study.

Data type	Sensor	Resolution	Row / column number	Number of images obtained
Landsat	TM	16d , 30 m	121/40	88
Landsat	ETM+	16d , 30 m	121/40	151
Landsat	OLI	16d , 30 m	121/40	60
MOD09A1	TERRA	8d , 500 m	121/40	847

Lake. Because that the electromagnetic energy in the near-infrared (NIR) wavelength can be strongly absorbed by water, the combination of green and near-infrared bands can distinguish water surface from most land features. Compared to other algorithms, the NDWI has been proven to be the most efficient in water surface detection (Jain et al., 2005). According to the principle, the index can be calculated as follows:

$$\mathrm{NDWI} = \frac{(\mathrm{DN})_{\mathrm{Green}} - (\mathrm{DN})_{\mathrm{NIR}}}{(\mathrm{DN})_{\mathrm{Green}} + (\mathrm{DN})_{\mathrm{NIR}}} \tag{1}$$

where $(\mathrm{DN})_{\mathrm{NIR}}$ and $(\mathrm{DN})_{\mathrm{Green}}$ indicate the DN value in the near-infrared (NIR) and green bands of remote-sensing imagery, respectively.

The range of calculated NDWI is -1 to $+1$. Among them, positive values represent water features, while zero or negative values reflect soil and terrestrial vegetation features (McFeeters, 1996). The accuracy of water body extraction is mainly reflected in the boundary of water and land. Usually, the extraction results based on NDWI are compared with measurement data or the classification results based on high-resolution images. In this study, an original high-quality Landsat image was randomly selected, and precise classification of water bodies was completed based on careful interpretation and supervised classification. Taking the image of May 25, 2017 as an example, the results show that the overall accuracy coefficient of water extraction based on NDWI can reach 98.4%, and the kappa coefficient is 0.964.

Based on the calculated NDWI image, we set the positive NDWI to 1 and the zero or negative NDWI to 0 to distinguish between inundation area and non–inundation area. Because the reconstructed inundation date set of the Poyang Lake has a temporal resolution of 8-days, annual inundation duration of the lake floodplain wetland can be finally calculated by overlapping 45 or 46 two-value images of NDWI data set in a year and multiplied by 8 days. Therefore, inundation frequency (IF) was defined as follows:

$$\mathrm{P_{IF}} = \frac{1}{8\mathrm{m}} \sum_{t=1}^{m} w_t \times 8 \times 100\% \tag{2}$$

$$w_t = \begin{cases} 1, \text{inundation} \\ 0, \text{non–inundation} \end{cases} \tag{3}$$

where m is the number of images in a time period (season, year), and w_t denotes the processed two-value of NDWI (0 or 1) of a pixel in a NDWI image.

2.4. Image fusion model

2.4.1. Fusion framework of ESTARFM

In this study, the Enhanced Spatial and Temporal Adaptive Reflectance Fusion Model (ESTARFM) proposed by Zhu et al. (2010) was applied to reconstruct continuous remote sensing image data with high temporal and spatial resolution. In contrast to the traditional image fusion methods, ESTARFM can effectively improve the accuracy of predicted fine-resolution reflectance, especially for heterogeneous landscapes.

The ESTARFM is a data fusion method based on a moving window that consider the auxiliary information obtained from adjacent pixels with similar spectral and the weight of these pixels themselves. According to the theory, four steps are required to implement the ESTARFM algorithm: (1) use two fine-resolution images to search for pixels similar to the central pixel in a local window; (2) calculate the weights of all similar pixels ($\mathrm{W_i}$); (3) determine the conversion coefficients $\mathrm{V_i}$ by linear regression; and (4) use $\mathrm{W_i}$ and $\mathrm{V_i}$ to calculate the fine-resolution reflectance from the coarse-resolution image at the prediction date:

$$\mathrm{F}(\mathrm{x_{w/2}}, \mathrm{y_{w/2}}, \mathrm{t_p}, \mathrm{B}) = \mathrm{F}(\mathrm{x_{w/2}}, \mathrm{y_{w/2}}, \mathrm{t_m}, \mathrm{B}) + \sum_{\mathrm{i=1}}^{\mathrm{N}} \mathrm{W_i} \times \mathrm{V_i} \times (\mathrm{C}(\mathrm{x_i}, \mathrm{y_i}, \mathrm{t_p}, \mathrm{B}) - \mathrm{C}(\mathrm{x_i}, \mathrm{y_i}, \mathrm{t_m}, \mathrm{B})) \tag{4}$$

where F and C denote the fine-resolution reflectance and coarse resolution reflectance respectively; $(\mathrm{x_{w/2}}, \mathrm{y_{w/2}})$ is the location of central pixel; w is the width of searching window; N is the number of similar pixels including the central "prediction" pixel; $(\mathrm{x_i}, \mathrm{y_i})$ is the location of ith similar pixel; B is image band; $\mathrm{W_i}$ is the weight of ith similar pixel; $\mathrm{V_i}$ is conversion coefficient; $\mathrm{t_m}$ is the acquisition date for the fine-resolution images, and $\mathrm{t_p}$ is the corresponding date for fine-resolution images to be predicted.

The weight $\mathrm{W_i}$ decides the contribution of ith similar pixel to predicting reflectance change at the central pixel. It is a combined weight determined by spectral similarity and distance difference based on the following equations:

$$\mathrm{W_i} = (1 \Big/ \mathrm{D_i}) \Big/ \sum_{\mathrm{i=1}}^{\mathrm{N}} (1/\mathrm{D_i}) \tag{5}$$

$$\mathrm{D_i} = (1 - \mathrm{R_i}) \times \mathrm{d_i} \tag{6}$$

$$\mathrm{d_i} = 1 + \sqrt{(\mathrm{x_{w/2}} - \mathrm{x_i})^2 + (\mathrm{y_{w/2}} - \mathrm{y_i})^2} \Big/ (\mathrm{w} \Big/ 2) \tag{7}$$

where R_i is the spectral correlation coefficient between fine- and coarse-resolution pixel for *i*th similar pixel. More detailed information about the ESTARFM algorithm can refer to Zhu et al. (2010).

The flowchart of the fusion process ESTARFM is shown in Fig. 3. According to the figure, the ESTARFM fuses and reconstructs Landsat images of the current day (L_p) through a MODIS image (M_p) of the simulation date and Landsat (L_a, L_b) and MODIS (M_a, M_b) images of at least two periods before and after the simulation date. Concurrent MODIS and Landsat images in the same year were chosen to make up a pair. If this criterion was not met, another Landsat image with the closest date in the previous or next year was chosen as an alternative.

2.4.2. Fusion strategy and accuracy evaluation

Generally, there are two fusion schemes: BI (Blend-then-Index) and IB (Index-then-Blend), which differ in the fusion order. According to previous studies (e.g., Ye et al., 2019), the IB scheme can weaken the speckle phenomenon caused by cloud interference, and can better reflect the fine texture characteristics of real features. In this study, we selected the IB scheme for image fusion, that is, the input data in ESTARFM model is the calculated NDWI images.

Due to the limited amount of available Landsat data during the study period, we reconstructed a total of 667 missing NDWI dataset by using the ESTRAFM model based on the acquired Landsat and MODIS surface reflectance datasets, thus building a continuous high spatial and temporal resolution (8d, 30 m) NDWI dataset of Poyang Lake from 2000 to 2020. Fig. 4 shows the distribution of the time series of the reconstructed NDWI and the directly computed NDWI from actual Landsat images. The accuracy of the fusion model was verified by subtracting the extracted inundated area of the directly available Landsat images and the ESTARFM fused images of the same day. The results show that the accuracy coefficient (1-Total area of subtracted difference/Total area of the whole lake) of the fusion model in extracting inundated water surface from 299 high-quality Landsat images was between 87.6% and 97.3%, with an average accuracy of 92.7%. It should be pointed out that due to the limitations of the threshold value determination for water extraction using the NDWI method and the fusion method, uncertainties inevitably exist in the reconstructed NDWI data based on the ESTRAFM model.

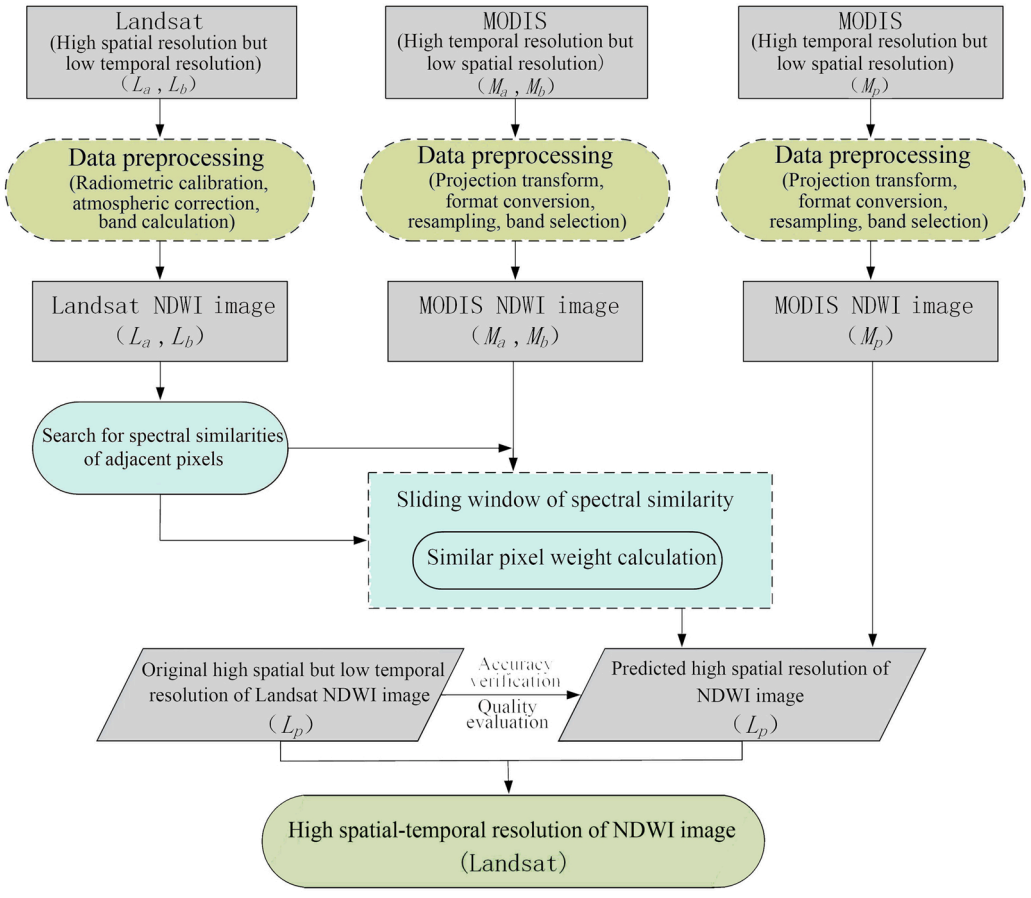

Fig. 3. Flowchart of ESTRAFM data fusion.

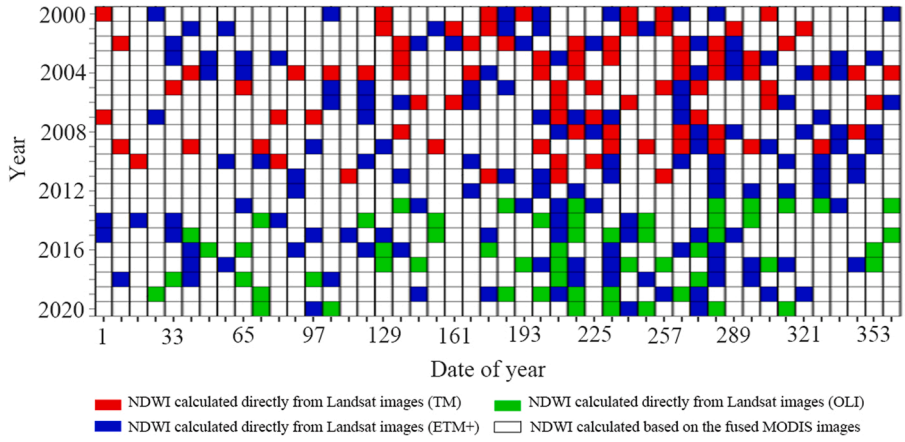

Fig. 4. Distribution of the reconstructed NDWI and the directly computed NDWI from actual Landsat images.

3. Results

3.1. Spatiotemporal heterogeneity of inundated area

The inundated area (IA) of the Poyang Lake showed remarkable monthly fluctuations in a year (Fig. 5). Normally, IA of the lake increases steadily in first half of the year from January to June, and reaches its peak in July. After that, IA of the lake gradually decreases in the following months. During the study period, the maximum IA of the lake exceeded 3100 km^2, and occurred in July 30, 2003, while the minimum IA was less than 400 km^2 in December 11, 2011. Monthly IA of the lake also shows great variability among years. The biggest variability of monthly IA was observed in October (2405 km^2) and the smallest was in July (990 km^2). Generally, lower variability of monthly IA mainly occurred in the winter dry season and the summer flood season. During these periods, IA of the lake usually reached the extreme value and changed little. In contrast, larger variability of monthly IA usually occurred in the spring season (April and May), when lake surface expanded rapidly, and in the autumn season, when the lake surface shrunk quickly (September and October).

The wide existence of interconnected dish-shaped temporary lakes in the floodplain is one of the most notable features of the Poyang Lake. Statistical result indicates that the annual average IA in the regions of MLR and FLR are 1232 km^2 and 392 km^2, respectively. Both show an overall similar seasonal fluctuations in the year, but the inundation details in some months are asynchronous. As shown in the gray areas in Fig. 6a, the asynchrony of IA mainly occurred at three different time periods. Firstly, at the end of March, when IA in the MLR showed an increasing trend, while decreasing was observed in the FLR. Secondly, in the beginning of July, when IA in the MLR continued to increase and reached the peak in a year, IA in the FLR decreased sharply. Thirdly, during the recession period of Poyang Lake in October, when IA in the FLR decreased rapidly at the beginning and maintained stable subsequently, the observed rapid decrease of IA in the MLR continued until November. Fig. 6b further indicates that the IA in the two regions showed opposite long-term change trend on an annual timescale. During the study period, IA in the MLR showed a weak decreasing trend, while it showed a slight increasing trend in the FLR. Their calculated Hurst indices are all greater than 0.5, indicating that there is long-term memory in the time series of inundated area.

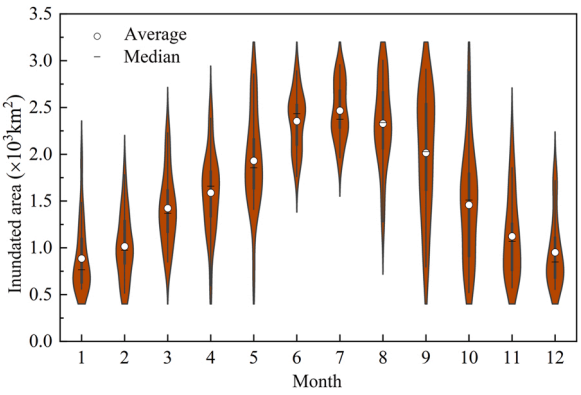

Fig. 5. Monthly variation of inundated area (IA) in the Poyang Lake during 2000–2020.

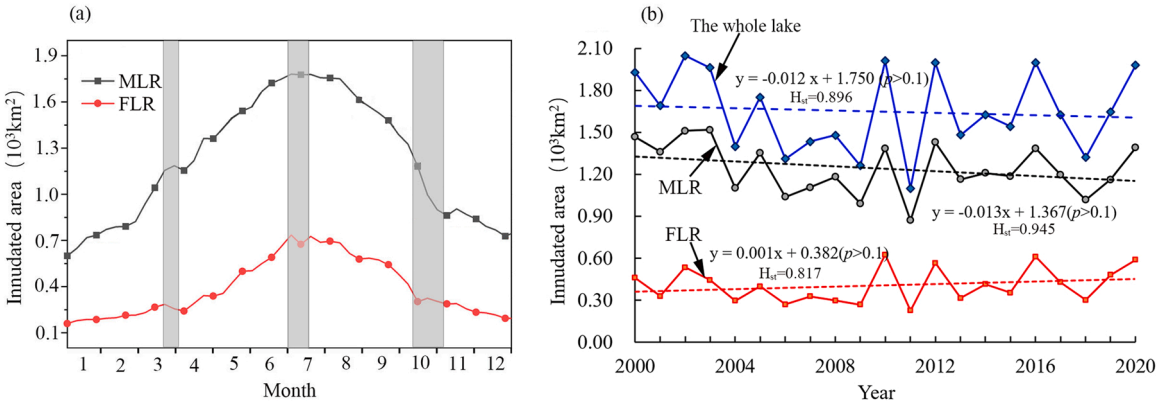

Fig. 6. Average intra-annual (a) and inter-annual (b) variations of inundated area (IA) in the main lake region (MLR) and floodplain temporary lakes region (FLR).

3.2. *Spatiotemporal heterogeneity of inundation frequency*

The annual average inundation frequency (IF) across the Poyang Lake shows significant spatiotemporal differences (Fig. 7). Spatially, IF of the Poyang Lake is generally high in the north and low in the south. Areas with particularly high IF are mainly concentrated in the north outflow channels and the northeast bay. IF in these areas is close to 60–90%, and some places are permanently inundated. In contrast, areas with low IF are mostly distributed in the delta fronts of inflow rivers in the southeast and southwest of the lake floodplain, where IF is mostly less than 40%. However, in these areas, most of the isolated dish-shaped temporary lakes show a status of high IF. The IF in the dish-shaped temporary lakes gradually decreases from the center to the edge, and spatially unevenly patched across the floodplain region (Fig. 7a). Some of the isolated artificial temporary lakes, such as Banghu, Dahuchi, Dchahu in the southwest of Songmen Mountain, and Jinxihu, Yangfanghu and Qinglanhu in the south, have very high IF values and stable spatial distribution because of relatively closed condition and weak hydrological connection in the Poyang Lake.

IF in the whole Poyang lake varies seasonally. In spring (Mar-May), IF in the areas such as the northern outflow channels, the central part and the northeast bay is large, while IF in other areas is small (Fig. 7b). In summer (Jun-Aug), IA of the lake increases greatly, and lake surface gradually expands to the FLR. Meanwhile, IF in almost 60% area of the lake exceeding 80% (Fig. 7c). During the recession period in autumn (Sep-Nov), lake surface shrinks quickly to the center. Except for the northeast bay, areas with high IF mainly distributed along the river channels (Fig. 7d). Although the overall IF in the FLR decreases significantly, the IF remains high in most dish-shaped temporary lakes. After entering the dry season in winter (Dec-Feb), the Poyang Lake further shrinks. Except for the northeast bay, the IA of the lake is highly concentrated in the river channels, showing a narrow thready meander outlook (Fig. 7e). In this process, the floodplains of the Poyang Lake widely exposed, and most of the dish-shaped temporary lakes have dried up. The above seasonal inundation process indicates that the lake surface mainly expands from north to south and shrinks from south to north.

The inter-annual change trend of IF in the Poyang Lake also shows obvious spatial discrepancy. Generally, an increasing trend of IF was mainly observed in the FLR with low IF, while a decreasing trend of IF was mainly observed in the MLR with high IF (Fig. 8a). The linear rate of IF in the Poyang Lake ranges in − 0.146–0.151/a, and most areas show a decreasing trend (Fig. 8b). The area with significant increasing trend of IF accounts for about 17% of the whole lake, which mainly distributed in FLR. In addition, there is also a certain distribution along the outflow channels in the north. In contrast, the area with significant decreasing trend of IF accounts for about 33% of the whole lake, and mainly distributed in the center areas of MLR. For the two regions of FLR and MLR, statistical results demonstrate that IF increased in FLR, while decreased in MLR (Fig. 8c).

Fig. 9 shows the inter-annual variation of IF in the whole Poyang Lake, and the regions of main lake and floodplain temporary lakes. It is clear from the figure that the three lines show basically consistent annual fluctuation, and all reached the minimum value in 2011. With comparison to the MLR, the fluctuation amplitude of IF in FLR was relatively larger. During the study period, the IF of the whole Poyang Lake showed an insignificant decreasing trend. However, opposite change trends of IF were observed between the two regions of MLR and FLR: IF in the MLR showed a weak decreasing trend, while IF in the FLR showed a weak increasing trend. The calculated Hurst indices further indicate the persistence of the changing trends in the three regions.

3.3. *Relationship between inundation dynamics and lake water level*

The relationship between the inundation dynamics of Poyang Lake and lake water level shows strong spatiotemporal differences (Fig. 10). On monthly timescale, the linear correlations between IA and lake water level is highest in August-September, and the correlation coefficients are greater than 0.90. The lowest correlations mainly occur in January-March, and the correlation coefficients can less than 0.73. This correlation at Kangshan station shows the highest in September and October. Whereas, the correlation at other stations is better in August and September. On average, the Duchang station in the most center of the lake shows the highest linear correlation between IA and lake water level. This is also displayed on the 8-days timescale.

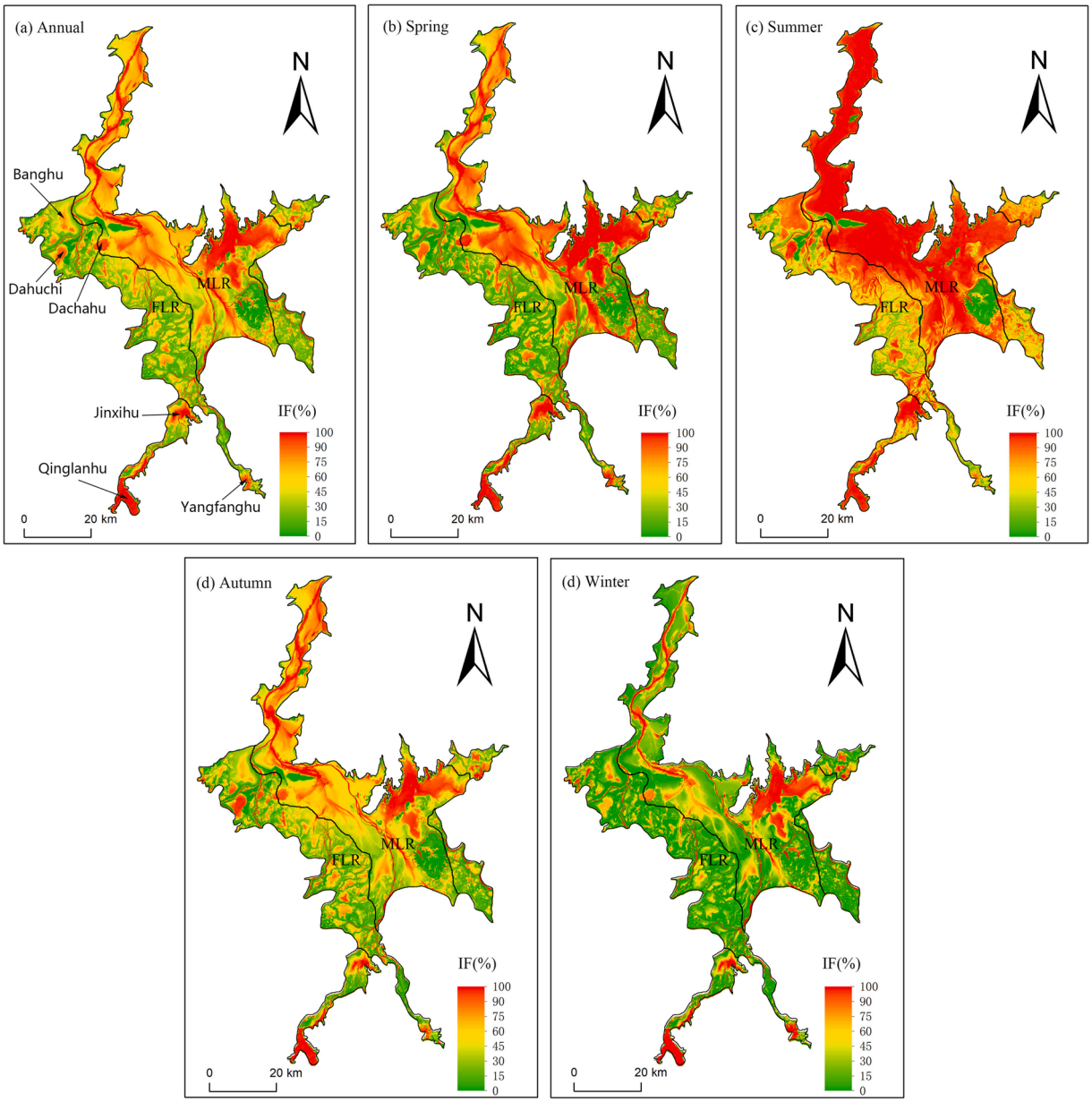

Fig. 7. Spatial distribution of annual and seasonal inundation frequency (IF) across the whole Poyang lake.

The correlation analysis of IF and lake water level at different hydro-stations was conducted on the seasonal timescale (Fig. 11). The result shows that the linear correlation between the two variables is highest in summer, followed in spring and autumn, while worst in winter. On the annual timescale, this correlation shows the highest at Duchang station in the center of the lake and gradually deviated towards the upstream and downstream ends of the lake.

4. Discussion

4.1. Impacts of human activities on the lake inundation dynamics

The IA in MLR and FLR shows obvious asynchronous fluctuations in two periods in spring and autumn seasons (Fig. 6a), which is mainly attributed to the human disturbance in the FLR. The Poyang Lake is rich in fish resource, which has nurtured people around the lake for generations and formed a unique way of fishing and management. Normally, during the recession period of the lake in autumn, when the inundated floodplain fades, wetlands gradually expose and large number of interconnected dish-shaped temporary lakes

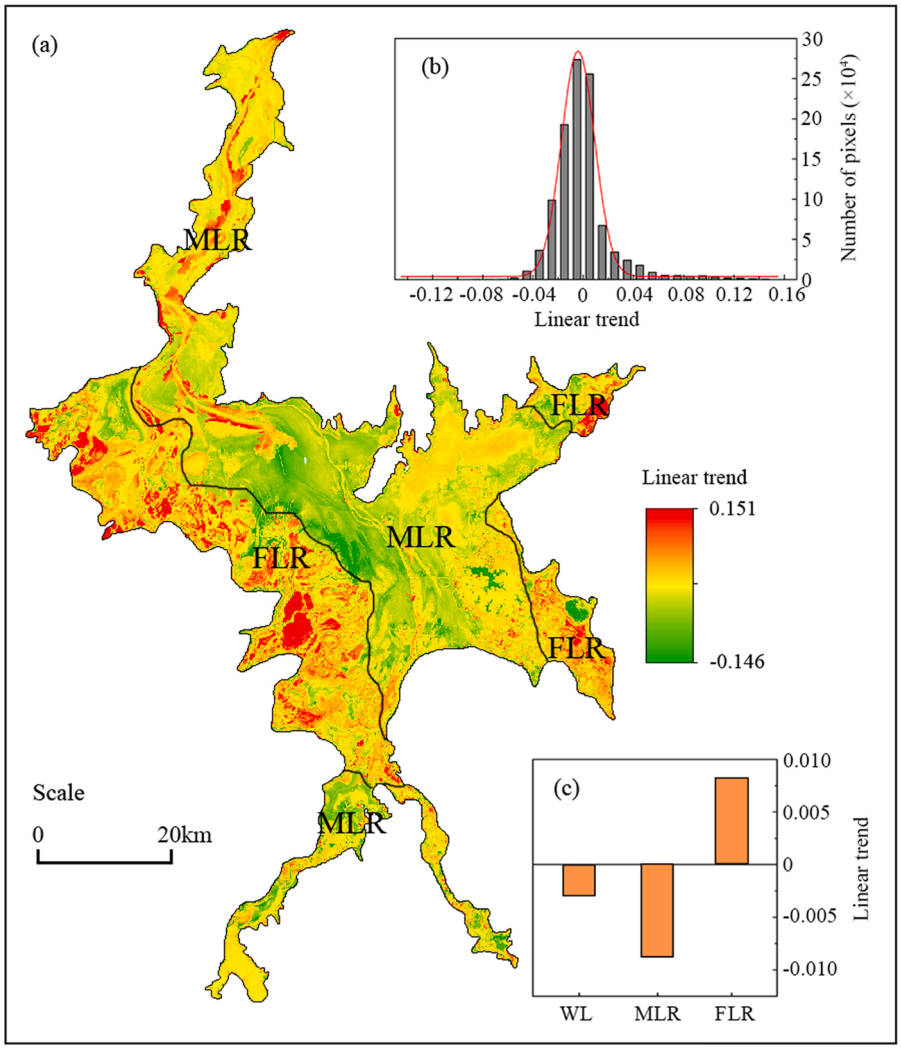

Fig. 8. Variation of inundation frequency (IF): (a) spatial distribution of linear trend of IF across the lake, (b) linear trend distribution of IF based on pixel statistics, and (c) difference of IF linear trend among the whole lake (WL), main lake region (MLR) and floodplain temporary lakes region (FLR).

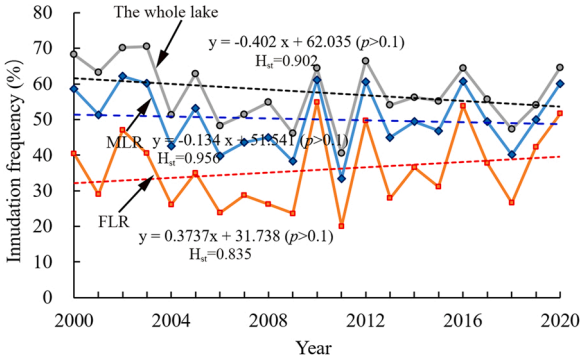

Fig. 9. Inter-annual variation of inundation frequency (IF) in the whole lake (WL), main lake region (MLR) and floodplain temporary lakes region (FLR).

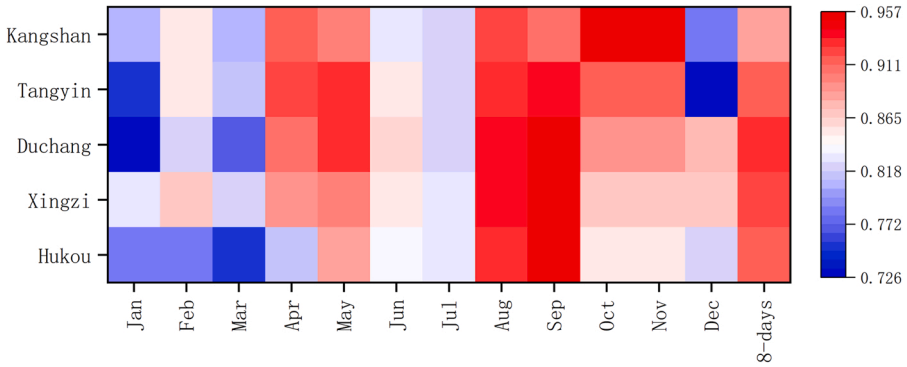

Fig. 10. Monthly correlation of inundated area and lake water level at different hydro-stations.

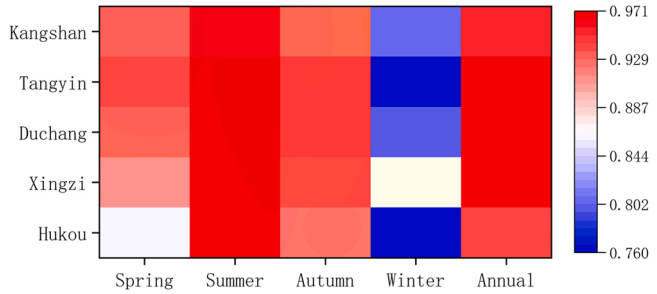

Fig. 11. Monthly correlation of inundation frequency and lake water level at different hydro-stations.

emerge. By using the topography characteristics of dish-shaped temporary lakes and the regime of seasonal fluctuation of lake water level, some of the dish-shaped temporary lakes were enclosed (dug, terraced, dammed, or surrounded by low embankments) and farmed by local fishermen (Guo et al., 2014). This will lead to a relative increase of the water surface in FLR, with reference to the

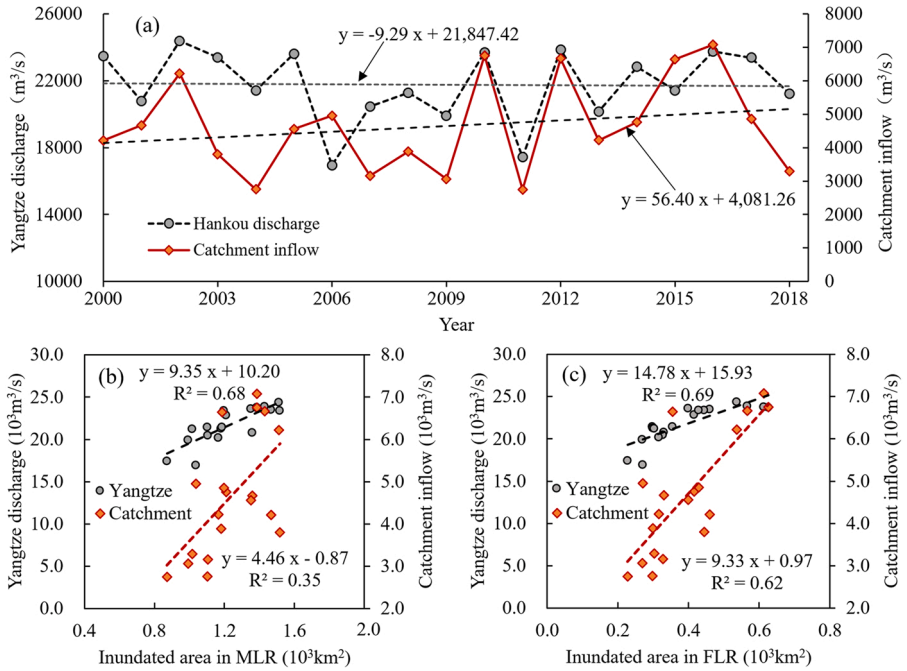

Fig. 12. (a) Annual variation of runoff for the Yangtze River (measured at Hankou station) and the Poyang Lake catchment during 2000–2018, and their correlations with the inundated area in (b) the MLR and (c) the FLR.

inundation change in MLR. However, during April in the spring season, a large number of the enclosed dish-shaped temporary lakes are released in advance by local fishermen before the rise of lake water level, resulting in an abnormal reduction of IA in FLR during this period. Due to the lack of inundation data with high spatial-temporal resolution, this result has not been reported in previous studies (e.g. Wu and Liu, 2015; Tan et al., 2019).

In addition, the main reason for the increasing trend of IF along the outflow channel in the northern part of MLR (as shown in Fig. 8a) lies in the enlargement of outflow channel caused by sand mining activities in the lake (Ye et al., 2020).

4.2. Driving causes for the inter-annual change trends

The hydrological complexity of the Poyang Lake lies in that it receives water from its catchment, while is directly affected by the Yangtze River. Normally, the Yangtze River discharge (at Hankou Station) peaks 1–2 months later than the catchment inflow of Poyang Lake. Therefore, before the peak of catchment inflow, the lake water level rises quickly, resulting in the strong outflows from Poyang Lake to the Yangtze River and forming a massive lake force (Guo et al., 2012). However, after the peak of catchment inflow, the so-called 'blocking effect' of the Yangtze River enhanced and creates a downstream control on lake water levels (Hu et al., 2007; Zhang et al., 2014). Previous studies have revealed that the rising period of lake water level from April to June is mainly controlled by the catchment inflow, while the recession period from July to September is mainly affected by the stage of the Yangtze River. Both the forces significantly weakened from October to March in next year, but relatively the effect of the Yangtze River is stronger during October-November, and the Poyang Lake is stronger in the next months (Hu et al., 2007; Guo et al., 2011; Zhang et al., 2014).

On an annual timescale, the variation of IA and IF in the MLR and FLR corresponds well to the variation of runoff from the Yangtze River and the lake catchment. During the past 20 years, runoff of the Yangtze River showed a slight decreasing trend, while the total runoff of the Poyang Lake catchment showed a slight increasing trend (Fig. 12a). Correlation analysis shows that the IA in MLR has a close relationship with the Yangtze River discharge, but has a relatively poor relationship with catchment inflow (Fig. 12b). In contrast, the IA in FLR is highly correlated with both the Yangtze River discharge and the catchment inflow, although the correlation with Yangtze River discharge is marginally higher (Fig. 12c). This result also demonstrates that the impact of catchment inflow on the inundation dynamics in FLR is relatively enhanced due to the higher position in the Poyang Lake, while the impact is relatively weakened in MLR because of lower position and direct connection with the Yangtze River. However, it is worth noting that the decreasing runoff in the Yangtze River is only one of the reasons for the decreasing trend of IA and IF in the MLR. The weakening 'blocking effect' of the Yangtze River due to intensive sand mining in the lake (Ye et al., 2020) and the operation of Three Gorges Dam in the upper stream of Yangtze River (Guo et al., 2012; Zhang et al., 2014) in recent years also added to the complexity of this driving mechanism.

The two influencing factors are intertwined and behave differently in different regions, resulting in obvious spatiotemporal heterogeneity of the inundation dynamics in the Poyang Lake. Given the significant spatial difference of IF between different regions of floodplain lakes, it is recommended that hydrological studies and water management plans should not be based on a general overview of inundation conditions of the entire ecosystem. Furthermore, this study revealed that the IF of the whole Poyang Lake showed an insignificant decreasing trend, while opposite change trends of IF were observed between the two regions of MLR and FLR. This suggests that the contrasting trends in the MLR and FLR are not detected when assessing the whole lake, which potentially results in an inaccurate assessment of no-trend.

4.3. Potential significance of the stage-area relationship in floodplain lakes

The stage-area relationship is one of the basic characteristics of lake hydrology. This relationship is usually incorporated in lumped-parameter management models of lake system (Zhang and Werner, 2015). The results of this study indicate that, for large shallow floodplain lakes, the linear characteristics of stage-area relationship also have obvious spatiotemporal heterogeneity. The relationship of a single hydrological station is difficult to be applied to other areas in the lake. Because the Duchang station is located at the most center of the lake, the relative effect of the Yangtze River and the catchment inflow on the lake reaches a relative equilibrium state here, and so the linear relationship between the lake water level and IA is relatively stable. The relationship gradually deviated towards the upstream and downstream ends of the lake. Therefore, for large open lakes, by considering the relative impacts of catchment inflow and the lake connected river, the stage-area relationship at the central station along the flow direction of the lake may be more meaningful for predicting lake water surface/volume under given water levels.

5. Conclusions

Inundated area of large floodplain shows significant seasonal fluctuation and monthly variability. Lower variability of lake surface mainly occurs in the periods when inundated area reaches the extremes (maximum or minimum). However, larger variability usually occurs in the periods when lake surface expands or shrinks rapidly. It is found that within the same floodplain lake, the inundated area and inundation frequency in different regions of the lake (the main lake region and the adjacent floodplain region) can present asynchronous intra-annual fluctuation and opposite inter-annual change trend. Spatially, the deviated stage-area linear relationship is common and significant in large floodplain lakes. The stage-area relationship at the central station along the flow direction of the lake is considered to be the most representative. The background driving mechanism for the spatiotemporal heterogeneity of inundation dynamics in large floodplain lakes mainly lies in the hydrological openness of such lakes. The changing counter-balance between the two forces of the lake catchment inflow and the lake-connected river (Yangtze River) in different regions of the lake play a combined

effects on lake inundation processes. Human activities, such as the fishing management in the floodplains and sand mining induced change of lake bathymetry also added to the hydrological complexity in different regions.

The use of spatiotemporal fusion models can accurately extract the inundation area of floodplain lakes. However, the selection of different fusion models may also have a certain impact on the accuracy of the final results. Although fusion accuracy of the ESTRAFM model in our case study is high, there is no detailed comparison of the result of different fusion models. Subsequent studies can consider comparing the accuracy of multiple fusion models to make the fusion results more convincing. In addition, based on the constructed high spatiotemporal resolution inundation dataset, the spatial patterns of water depth hydrological connectivity in these floodplain areas can be calculated, which are particularly essential for the prediction of wetland vegetation change and the evaluation of ecosystem stability in future studies.

The findings of this study extend the understanding of the hydrological complexity of large heterogeneous floodplain systems, which have broader impacts for eco-hydrological research and management of relevant floodplain areas worldwide. In light of the significant spatial difference of lake inundation dynamics, especially between the main lake and adjacent floodplains, plans of water resources management and ecological protection should be implemented differently in different regions of the lake system. Because that spatially deviated stage-area relationship is common and significant for large heterogeneous floodplain lakes, it is necessary to incorporate multi-site non-linear relationship analysis in the prediction of lake inundation.

CRediT authorship contribution statement

Xuchun Ye: Conceptualization, Methodology, Investigation, Writing – original draft, Funding acquisition. **Juan Wu:** Data curation, Visualization, Writing – review & editing. **Xianghu Li:** Validation, Writing – review & editing, Funding acquisition. **Yunliang Li:** Data supporting, Validation. **Qi Zhang:** Supervision, Resources. **Chong-Yu Xu:** Writing – review & editing.

Declaration of Competing Interest

The authors declare that they have no known competing financial interests or personal relationships that could have appeared to influence the work reported in this paper.

Data Availability

Data will be made available on request.

Acknowledgements

This work was jointly funded by the National Key Research and Development Program of China (grant number 2022YFC3204102), the National Natural Science Foundation of China (grant number 42071028), the Ganpo Excellent Talent Support Program of Jiangxi–Training Program for Academic and Technical Leaders in Major Disciplines (grant number 20232BCJ22011) and the Jiujiang Science and Technology Innovation Talent Project (grant number S2022QNZZ056). We are grateful to the editor and two anonymous reviewers for the constructive suggestions given during the review process.

Appendix A. Supporting information

Supplementary data associated with this article can be found in the online version at doi:10.1016/j.ejrh.2023.101541.

References

Allen, Y., 2016. Landscape scale assessment of floodplain inundation frequency using Landsat imagery. River Res. Appl. 32 (7), 1609–1620. https://doi.org/10.1002/rra.2987.

Alsdorf, D.E., Rodriguez, E., Lettenmaier, D.P., 2007. Measuring surface water from space. Rev. Geophys. 45, RG2002. https://doi.org/10.1029/2006RG000197.

Casanova, M.T., Brock, M.A., 2000. How do depth, duration and frequency of flooding influence the establishment of wetland plant communities? Plant Ecol. 147 (2), 237–250. https://doi.org/10.1023/A:1009875226637.

Cazenave, A., Milly, P.C.D., Douville, H., Benveniste, J., Kosuth, P., Lettenmaier, D., 2004. Space techniques used to measure change in terrestrial waters. EOS Trans. 85 (6), 59. https://doi.org/10.1029/2004EO060006.

Coops, H., Hosper, S.H., 2002. Water-level management as a tool for the restoration of shallow lakes in the Netherlands. Lake Reserv. Manag. 18 (4), 293–298. https://doi.org/10.1080/07438140209353935.

Coops, H., Beklioglu, M., Crisman, T.L., 2003. The role of water-level fluctuations in shallow lake ecosystems–workshop conclusions. Hydrobiologia 506 (1–3), 23–27. https://doi.org/10.1023/B:HYDR.0000008595.14393.77.

Finlayson, M., Harris, J., McCartney, M., Lew, Y., Zhang, C., 2010. In: Report on Ramsar visit to Poyang Lake Ramsar site, PR China. pp. 1–34 (Report prepared on behalf of the Secretariat of the Ramsar Convention, April 12–17. <http://www.ramsar.org/pdf/Poyang_lake_report_v8.pdf>).

Frappart, F., Bian, Ca Maria, S., Normandin, C., Blarel, F., Bourrel, L., Aumont, M., Azemar, P., Vu, P.-L., Le Toan, T., Lubac, B., Darrozes, J., 2018. Influence of recent climatic events on the surface water storage of the Tonle Sap Lake. Sci. Total Environ. 636, 1520–1533. https://doi.org/10.1016/j.scitotenv.2018.04.326.

Gronewold, A.D., Rood, R.B., 2019. Recent water level changes across Earth's largest lake system and implications for future variability. J. Gt. Lakes Res. 45 (1), 1–3. https://doi.org/10.1016/j.jglr.2018.10.012.

Gronewold, A.D., Bruxer, J., Durnford, D., Smith, J.P., Clites, A.H., Seglenieks, F., Fortin, V., 2016. Hydrological drivers of record-setting water level rise on Earth's largest lake system. Water Resour. Res. 52 (5), 4026–4042. https://doi.org/10.1002/2015wr018209.
Guo, H., Hu, Q., Zhang, Q., 2011. Changes in Hydrological interactions of the Yangtze River and the Poyang Lake in China during 1957-2008. Acta Geogr. Sin. 66 (5), 609–618. https://doi.org/10.1631/jzus.B1000185.
Guo, H., Hu, Q., Zhang, Q., Feng, S., 2012. Effects of the Three Gorges Dam on Yangtze River flow and river interaction with Poyang Lake, China: 2003-2008. J. Hydrol. 416, 19–27. https://doi.org/10.1016/j.jhydrol.2011.11.027.
Guo, H., Hu, B., Li, Q., 2014. Effects of autumn fishery by enclosing plate-shaped lake on the winter migratory birds and conservation strategies in Nanji wetland national natural reserve of the Poyang lake, jiangxi. Resour. Environ. Yangtze Basin 23 (1), 46–52.
Heimhube, V., Tulbure, M.G., Broich, M., 2017. Modeling multidecadal surface water inundation dynamics and key drivers on large river basin scale using multiple time series of Earth-observation and river flow data. Water Resour. Res. 53 (3), 1251–1269. https://doi.org/10.1002/2016wr019858.
Hu, Q., Feng, S., Guo, H., Chen, G., Jiang, T., 2007. Interactions of the Yangtze River flow and hydrologic processes of the Poyang Lake, China. J. Hydrol. 347, 90–100. https://doi.org/10.1016/j.jhydrol.2007.09.005.
Hudon, C., Wilcox, D., Ingram, J., 2006. Modeling wetland plant community response to assess water-level regulation scenarios in the Lake Ontario-St. Lawrence River basin. Environ. Monit. Assess. 113 (1–3), 303–328. https://doi.org/10.1007/s10661-005-9086-4.
Hui, F., Xu, B., Huang, H., Yu, Q., Gong, P., 2008. Modelling spatial-temporal change of Poyang Lake using multi-temporal Landsat imagery. Int. J. Remote Sens. 29 (20), 5767–5784. https://doi.org/10.1080/01431160802060912.
Jain, S.K., Singh, R.D., Jain, M.K., Lohani, A.K., 2005. Delineation of flood-prone areas using remote sensing techniques. Water Resour. Manag. 19, 333–347.
Koponen, J., Kummu, M., Sarkkula, J., 2005. Modelling environmental change in Tonle Sap Lake. Cambodia Int. Assoc. Theor. Appl. Limnol. 29 (Pt2), 1083–1086.
Li, Y., Zhang, Q., Yao, J., Werner, A.D., Li, X., 2014. Hydrodynamic and hydrological modeling of the Poyang Lake catchment system in China. J. Hydrol. Eng. 19, 607–616. https://doi.org/10.1061/(ASCE)HE.1943-5584.0000835.
Li, Y., Zhang, Q., Werner, A.D., Yao, J., Ye, X., 2017. The influence of river-to-lake backflow on the hydrodynamics of a large floodplain lake system (Poyang Lake, China). Hydrol. Process. 31, 117–132. https://doi.org/10.1002/hyp.10979.
Li, Y., Zhang, Q., Cai, Y., Tan, Z., Wu, H., Liu, X., Yao, J., 2019a. Hydrodynamic investigation of surface hydrological connectivity and its effects on the water quality of seasonal lakes: insights from a complex floodplain setting (Poyang Lake, China. Sci. Total Environ. 660, 245–259. https://doi.org/10.1016/j.scitotenv.2019.01.015.
Li, Y., Zhang, Q., Liu, X., Tan, Z., Yao, J., 2019b. The role of a seasonal lake groups in the complex Poyang Lake-floodplain system (China): insights into hydrological behaviors. J. Hydrol. 578, 124055 https://doi.org/10.1016/j.jhydrol.2019.124055.
Li, Y., Tan, Z., Zhang, Q., Liu, X., Chen, J., Yao, J., 2021. Refining the concept of hydrological connectivity for large floodplain systems: framework and implications for eco-environmental assessments. Water Res 195, 117005. https://doi.org/10.1016/j.watres.2021.117005.
Liu, W., Xie, C., Zhao, L., Li, R., Liu, G., Wang, W., Liu, H., Wu, T., Yang, G., Zhang, Y., Zhao, S., 2021. Rapid expansion of lakes in the endorheic basin on the Qinghai-Tibet Plateau since 2000 and its potential drivers. Catena 197, 104942. https://doi.org/10.1016/j.catena.2020.104942.
Liu, X., Zhang, Z., Zhang, J., Zhu, B., Tian, J., 2023. Projection of the potential distribution of suitable habitats for Siberian Crane (Grus leucogeranus) in the middle and lower reaches of the Yangtze River Basin. Front. Earth Sci. 11, 1193677 https://doi.org/10.3389/feart.2023.1193677.
Liu, Y., Wu, G., Zhao, X., 2013. Recent declines in China's largest freshwater lake: trend or regime shift? Environ. Res. Lett. 8 (014010), 9. https://doi.org/10.1088/1748-9326/8/1/014010.
Price, J.C., 1994. How unique are spectral signatures. Remote Sens. Environ. 49, 181–186. https://doi.org/10.1016/0034-4257(94)90013-2.
Rudorff, C.M., Melack, J.M., Bates, P.D., 2014. Flooding dynamics on the lower Amazon floodplain: 1. Hydraulic controls on water elevation, inundation extent, and river–floodplain discharge. Water Resour. Res. 50, 1–16. https://doi.org/10.1002/2013WR014091.
Sichangi, A., Makokha, G., 2017. Monitoring water depth, surface area and volume changes in Lake Victoria: integrating the bathymetry map and remote sensing data during 1993–2016. Model. Earth Syst. Environ. 3 (2), 533–538. https://doi.org/10.1007/s40808-017-0311-2.
Tan, Z., Zhang, Q., Li, M., et al., 2016. A study of the relationship between wetland vegetation communities and water regimes using a combined remote sensing and hydraulic modeling approach. Hydrol. Res. 47 (S1), 278–292. https://doi.org/10.2166/nh.2016.216.
Tan, Z., Li, Y., Xu, X., Yao, J., Zhang, Q., 2019. Mapping inundation dynamics in a heterogeneous floodplain: Insights from integrating observations and modeling approach. J. Hydrol. 572, 148–159. https://doi.org/10.1016/j.jhydrol.2019.02.039.
Tan, Z., Melack, J., Li, Y., Liu, X., Chen, B., Zhang, Q., 2020. Estimation of water volume in ungauged, dynamic floodplain lakes. Environ. Res. Lett. 15 (5), 054021 https://doi.org/10.1088/1748-9326/ab82cb.
Tan, Z., Li, Y., Zhang, Q., Guo, Y., Wang, X., Li, B., Wan, R., Wang, D., Wu, X., 2022. Progress of hydrological process researches in lake wetland: a review. J. Lake Sci. 34 (1), 18–37. https://doi.org/10.18307/2022.0104.
Wu, G., Liu, Y., 2015. Capturing variations in inundation with satellite remote sensing in a morphologically complex, large lake. J. Hydrol. 523, 14–23. https://doi.org/10.1016/j.jhydrol.2015.01.048.
Wu, H., Zeng, G., Liang, J., Chen, J., Xu, J., Dai, J., Sang, L., Li, X., Ye, S., 2017. Responses of landscape pattern of China's two largest freshwater lakes to early dry season after the impoundment of Three-Gorges Dam. Int. J. Appl. Earth Obs. 56, 36–43. https://doi.org/10.1016/j.jag.2016.11.006.
Yang, G., Ma, R., Zhang, L., Jiang, J., Zeng, H., 2010. Lake status, major problems and protection strategy in China. J. Lake Sci. 22 (6), 799–810. https://doi.org/10.1080/09500340.2010.529951.
Yao, X., Zhang, L., Zhang, Y., Xu, H., Jiang, X., 2016. Denitrification occurring on suspended sediment in a large, shallow, subtropical lake (Poyang Lake, China. Environ. Pollut. 219, 501–511. https://doi.org/10.1016/j.envpol.2016.05.073.
Ye, X., Zhang, Q., Liu, J., Xu, L., 2012. Natural runoff change characteristics and flood/drought disasters in Poyang Lake catchment. J. Natural. Disasters 21 (1), 140–147. https://doi.org/10.1007/s11783-011-0280-z.
Ye, X., Meng, Y., Xu, L., Xu, C.-Y., 2019. Net primary productivity dynamics and associated hydrological driving factors in the floodplain wetland of China's largest freshwater lake. Sci. Total Environ. 659, 302–313. https://doi.org/10.1016/j.scitotenv.2018.12.331.
Ye, X., Liu, F., Zhang, Z., Xu, C.-Y., 2020. Quantifying the Impact of Compounding Influencing Factors to the Water Level Decline of China's Largest Freshwater Lake. J. Water Res. Plan. Man.146(6), 05020006. https://doi.org/10.1061/(ASCE)WR.1943–5452.0001211.
Zedler, J.B., Kercher, S., 2005. Wetland resources: status, trends, ecosystem services and restorability. Ann. Rev. Environ. Resour. 30, 39–74. https://doi.org/10.1146/annurev.energy.30.050504.144248.
Zhang, J., Chu, L., Zhang, Z., Zhu, B., Liu, X., Yang, Q., 2023. Evolution of small and micro wetlands and their driving factors in the Yangtze River Delta - a case study of Wuxi area. Remote Sens. 15, 1152. https://doi.org/10.3390/rs15041152.
Zhang, Q., Werner, A.D., 2015. Hysteretic relationships in inundation dynamics for a large lake–floodplain system. J. Hydrol. 527 (4), 160–171 https:// doi.org/10.1016/j.jhydrol.2015.04.068.
Zhang, Q., Ye, X., Adrian, D.W., Li, Y., Yao, J., Li, X., Xu, C.-Y., 2014. An investigation of enhanced recessions in Poyang Lake: comparison of Yangtze River and local catchment impacts. J. Hydrol. 517, 425–434. https://doi.org/10.1016/j.jhydrol.2014.05.051.
Zhu, X., Jin, C., Feng, G., Chen, X., Masek, J.G., 2010. An enhanced spatial and temporal adaptive reflectance fusion model for complex heterogeneous regions. Remote Sens. Environ. 114 (11), 2610–2623. https://doi.org/10.1016/j.rse.2010.05.032.